JOURNAL OF MATERIALS SCIENCE 25 (1990) 4186–4193

The bonding mechanism of aramid fibres to epoxy matrices

Part 1 *A review of the literature*

J. KALANTAR, L. T. DRZAL
Department of Chemical Engineering, and Composite Materials and Structures Center, Michigan State University, East Lansing, Michigan 48824-1326, USA

Despite considerable attempts to increase aramid–epoxy adhesion, to date, the adhesion levels achieved between aramid fibres and epoxy matrices are less than optimum for some applications. A combination of the aramid fibres' morphology, physical and chemical properties, and the interfacial mechanical stresses is responsible for the lack of success in increasing aramid–epoxy adhesion level. A key to improving the aramid–epoxy adhesion is a basic understanding of the interfacial mechanisms by which fibre and matrix interact. There is a considerable number of publications on aramid fibres and their composites. This paper reviews some of the literature relevant to aramid–epoxy bonding mechanisms.

1. Introduction

Aramid fibres are viable constituents for advanced composite materials offering alternative and complementary properties to those of inorganic reinforcements such as glass and carbon fibres. The combination of stiffness, high strength, high fracture strain, and low density of the aramid fibres is unmatched by inorganic reinforcing fibres. Advanced composites made from aramid fibres have comparable axial properties to inorganic fibre-reinforced composites, as well as significant reduction in weight. However, the off-axis properties of aramid composites are limited by low fibre–matrix adhesion compared to inorganic fibre-reinforced composites. High levels of fibre–matrix adhesion are required for achieving optimum off-axis composite properties. Increasing aramid–matrix adhesion may also improve the compressive strength of aramid composites by deterring the onset of fibre buckling [1].

This report reviews the current literature on adhesion-related properties of aramid fibres. Extended discussions on aramid fibres, their composite properties, and their morphology are provided in recent review articles by Morgan *et al.* [2], Chiao *et al.* [3], and Chatzi and Koenig [4].

2. Composite interphase

A composite interphase is the region between fibre and matrix with different chemical and physical properties from those of fibre and matrix [5]. The mechanical behaviour of composite materials reflects the interactions between their various constituents. When a load is applied to a fibre-reinforced composite, the load is transferred between matrix and fibre through their interphase. A strong interphase promotes greater involvement of the fibres, thus increasing the composite strength. The condition of the interphase also determines the failure mode of the composite. At high levels of adhesion, failure initiates with matrix cracks, but at lower adhesion levels, failure occurs along the fibre–matrix interface. Increasing interfacial adhesion can improve off-axis properties such as interlaminar shear and transverse strength as well as environmental stability of polymeric composites [6]. For some applications such as fracture toughness, however, a low level of fibre–matrix adhesion is desirable. In general, the optimum condition for the interphase depends on the particular application and its expected loads.

In elementary treatments of composite properties, effects of the interphase are usually ignored [7]. In practice, the interphase has moderate to critical influences on many mechanical and thermal properties of the composite [5]. Studies by Drzal *et al.* [8] and Owen [9] on carbon fibres with different surface properties have demonstrated the significance of the interphase on composite properties. Peters and Springer [10] have shown that the mechanical properties of the composite are affected more by the fibre–matrix interphase than by the degree of the cure of the matrix. Such observations suggest that optimizing the curing cycles of the resin should be with respect to both the desired fibre–matrix interphase and the optimum matrix mechanical properties.

At low levels of fibre–matrix adhesion, the interphase can act as a buffer against impact and improve fracture toughness and impact resistance of the composites. A report by Chang *et al.* [11] on carbon–epoxy composites with controlled interphase has shown an inverse relation between interlaminar shear strength and impact resistance of the composites. Similar work by Mai and Castino [12] on fracture toughness of Kevlar–epoxy composites has demonstrated a 200% to 300% greater fracture toughness for Estapol-7008 coated fibres than untreated fibres, showing that a very high level of fibre–matrix adhesion can be

0022-2461/90 $03.00 + .12

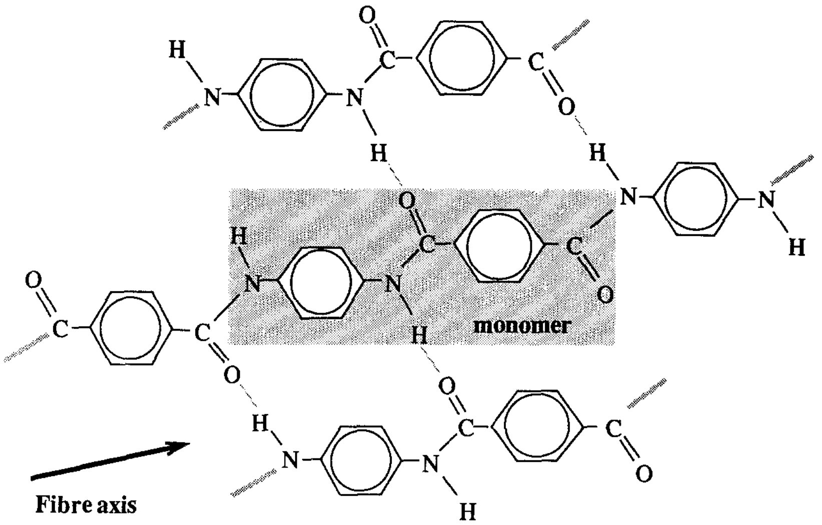

Figure 1 Structure of the PPTA polymer.

detrimental to fracture toughness and impact resistance of the composites.

3. Polyaramid fibres

At molecular levels, the strength of organic polymers is related to the rupture of their backbone chain. In theory, the material strength can be calculated from the dissociation energy of primary and secondary bonds and the packing of the polymers [13]. However, for most solid materials, the measured strength of the bulk material is much smaller than the theoretical values. The main reason is the existence of flaws or defects in the structure of the material. Misalignment in the orientation of the polymer chains, broken chain ends, and slippage of the chains can lead to stress concentrations which cause chain rupture and catastrophic failures. To reach high material strengths, a highly ordered polymer morphology and a high degree of crystallinity is required. Polymer chain packing, orientation, and extension significantly affect the material strength. The distribution of flaws and cracks which are detrimental to the strength must also be minimized. Termonia and Smith [14] have examined a theoretical evaluation of the stress–strain curve and ultimate mechanical properties of the polyaramid fibres. They have modelled the fibre as a three-dimensional array of primary and secondary bonds which are in a state of constant thermal vibration. A Monte-Carlo process simulates the thermally activated bond breakages. This model can predict time and temperature dependence of fibre tensile strength.

During the past two decades, considerable progress has been made in the production of high-performance synthetic fibres [15, 16]. These fibres have high degrees of crystallinity and their ultimate properties approach their theoretical maxima. The most successful high-performance organic fibres have been prepared from wholly aromatic polymers [17]. These fibres have high modulus, high strength, and are ductile. Preston [18] has reviewed the development of aromatic polymer fibres.

To date, the most successful high-performance organic fibres have been polyaramid fibres. E.I. du Pont is the major manufacturer of one type of polyaramid fibre which is marketed under the trade name "Kevlar®". Since its introduction in 1971, Kevlar has become the major reinforcing fibre for applications where toughness and impact resistance is required [19, 20]. Four types of Kevlar fibres are available for specific applications: (1) tyre cord Kevlar; (2) intermediate modulus Kevlar 29 for ropes and fabrics; (3) high modulus Kevlar 49 for composite reinforcement; and (4) the new Kevlar 149 with 40% higher modulus than Kevlar 49 [21]. Other examples of polyaramid fibres are "Twaron®" by Enka, and "Technora®" by Teijin Ltd.

Kevlar fibres consist of extended chains of highly oriented rod-like molecules formed into fibres with a nominal diameter of 12 μm. The aramid monomer is para-phenylene terephthalamide (PPTA) (Fig. 1). The polymer chains are oriented in the fibre longitudinal direction and are hydrogen bonded to each other.

A fibre fabrication process for the aramid fibres has been reported by Morgan and Allred [2]. Aramid fibres are produced by the condensation polymerization of terephthaloyl chloride and *p*-phenylene diamine. The PPTA is polymerized using a stoichiometric ratio of the reactants. The HCl formed during polymerization is neutralized with an NaOH wash. The PPTA polymers are then dissolved in a concentrated H_2SO_4 solvent to produce low-viscosity PPTA liquid crystalline dopes for the fibre fabrication. The solution ($\sim$ 20 wt % PPTA) is extruded at 80° C from spinneret orifices into fibre form. The resulting yarns are neutralized with NaOH and water washed to remove the resulting Na_2SO_4 salt. Subsequent drying, stretching, and drawing treatments increase the fibre stiffness and strength. The structure of Kevlar fibres is not firmly established, but some conclusions about its morphology can be made.

Dobb *et al.* [22], using electron diffraction and electron microscope dark-field image studies, have reported that the structure of Kevlar 49 fibre consists of sheets of polymer chains radially arranged and held together by hydrogen bonding (Fig. 2). These sheets are regularly pleated along the axial direction of the fibre, with a pleat angle of about 170°. Over small transitional sections between the pleated sheets, the PPTA polymers are parallel to the axial plane; this feature eliminates the possibility of rotational molecular orientation. Dobb *et al.* have observed 250 and 500 nm periodicities in the fibres, but near the edges

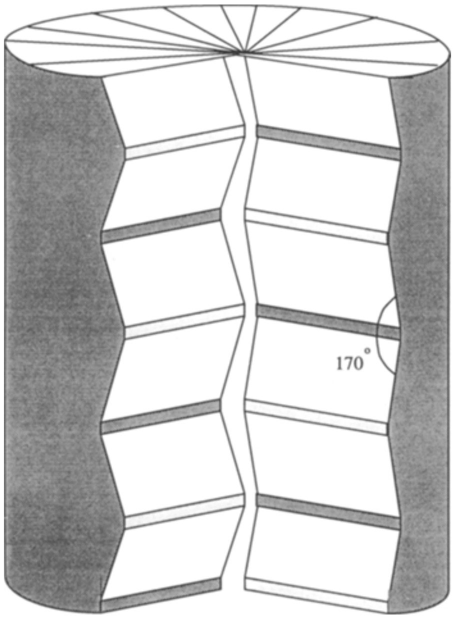

Figure 2 Dobb *et al.'s* [22] model for the polyaramid fibre structure. Diagram shows a system of radially pleated polymer planes. A small vertical section is located between each pleat.

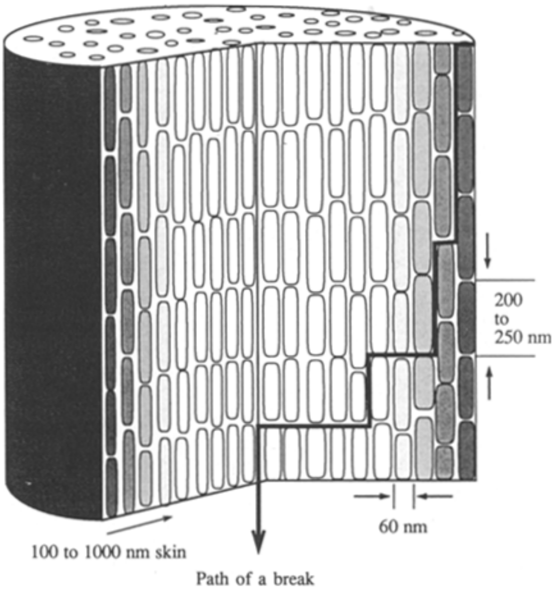

Figure 3 An exaggerated view of the aramid fibre morphology model proposed by Morgan *et al.* [23]. The PPTA chains are randomly distributed in the fibre exterior and progressively more clustered in the interior. This morphology results in skin–core differences in the fibre.

they have reported evidence of marked changes in this spacing. The change in the periodicity near the fibre exterior suggests a fibre skin with a different morphology from the core.

Morgan *et al.* [23] have studied the relation between Kevlar fibre failure processes and its structure. Based on the physical structure, fibre fabrication process, microscopic deformation and failure processes, and fracture topography of the etched fibres, they have proposed a model of chain-end distribution in a PPTA fibre. While not disputing the pleat morphology of the fibre, they have suggested that concentration and distribution of the PPTA macromolecular chain ends are the primary structural factors which affect deformation, failure, and strength of PPTA fibres. In this model (Fig. 3) chain-end distributions are random in the fibre exterior, but progressively more aligned and clustered in the fibre interior. The model also suggests a skin–core morphology for the fibre with random chain-end distribution at the skin and periodic weak planes in the core. The periodicity of the weak planes is about 200 nm, which is the suggested average length of a PPTA macromolecule rod. The periodic weak planes are sites of maximum chain-end concentration, but a large percentage of macromolecules pass through the weak planes ensuring fibre continuity in the axial direction. Morgan *et al.* further suggest that the fibre core consists of PPTA macromolecules which are clustered into crystal rods having a 60 nm diameter and a 200 nm length. It can be inferred from this model that crack propagation can readily occur parallel to the rods or across the weak planes, resulting in fibre fibrillations upon fracture.

The presence of internal weak planes within the fibre has been supported by the work of Brown *et al.* [24]. Their electron paramagnetic resonance studies have determined that the concentration of the stress-induced free radicals is more than the estimated concentration for the fracture surface. They have suggested that the excess free radicals are produced by polymer chain scission at weak planes within the fibre. Using ultramicrotomy, ion-thinning, and brittle fracture techniques, Li *et al.* [25] have demonstrated the crystallite layer morphology of the aramid fibres. They have also suggested that there are longer crystallites which pass through two or more layers. These long crystallites significantly strengthen the fibre along its axial direction because they transverse the internal weak planes.

There is numerous additional evidence supporting the skin–core morphology of the aramid fibres. Chatzi *et al.* [26], using photoacoustic Fourier transform infrared (FTIR) spectroscopy have determined a difference in the chain orientation between the exterior and the interior of the Kevlar 49 fibres. A strain bifringence study of aramid fibres by Yang *et al.* [27] has shown structural rearrangement by the aramid fibres in the initial stage of straining. They have attributed their observation to fibre inhomogeneity resulting from a skin–core orientation gradient. (ATR*)-FTIR studies by Tiefenthaler and Urban [28] have shown that the orientation of the surface species changes as the aramid surface is altered by hydrolysis. Electron microscopy studies by Li *et al.* [25] have also demonstrated the presence of the skin–core morphology of the aramid fibres.

The skin–core morphology of the aramid fibres can be due to its extrusion and coagulation process [2, 4]. During PPTA dope extrusion, shear forces cause the PPTA liquid crystals adjacent to the orifice wall to orient in the direction of shear and subsequent exposure to the coagulation bath quenches the fibre exterior.

In another report by Morgan and Pruneda [29], the chemical impurities in Kevlar 49 fibres have been investigated. They have determined that there are about 1.5 wt % impurities of which half are in the form of Na_2SO_4 which is the result of the sulphuric acid

---

*Attenuated total reflectance.

neutralization step. Similar impurity concentrations have been reported by Penn and Larsen [30]. Morgan has suggested that Na_2SO_4 residues in the interfibrillar regions are paths for moisture diffusion, which during fibre fabrication can generate microvoids in the fibre. Whalley *et al.* [31] have confirmed the possibility of an Na_2SO_4 hydration fracture mechanism from the analogy of "salt-weathering" mechanisms in geology. Small-angle X-ray scattering studies by Lee *et al.* [32] have suggested that failure of Kevlar 49 fibres is due to increases in the volume fraction of microvoids and their enlargement along the fibre axis direction. Ashbee and Ashbee [33] have proposed a chemical volume expansion model to describe the hydration expansion which can result in fibre fracture.

4. Aramid–epoxy adhesion

Separation of aramid fibres from an epoxy matrix is characterized by bare fibres with little resin adhering to them. The failure mode of the aramid–epoxy composites are generally interfacial [34, 35], with some surface fibrillation. Significant amounts of research have been devoted to the determination of the interfacial properties of glass and carbon fibres and many surface treatment techniques and coupling agents have been developed. For glass and carbon fibres these surface treatment techniques can increase the fibre–matrix adhesion by a factor of two or three [6, 36, 37]. Development of similar improvements with interfacial treatment methods for the aramid-reinforced composites has been difficult.

Cooke [38], Morgan and Allred [2] have documented various attempts for the development of surface treatment techniques for the aramid fibres. Despite many efforts, promising coupling agents have not yet been developed [39]. Surface treatments such as surface oxidation and etching techniques can improve adhesion, but are usually accompanied by losses in fibre tensile strength [40, 41]. A Kevlar 49 plasma treatment has been reported by Allred *et al.* [42]. Using a r.f. plasma in the presence of ammonia gas, Allred has reported a two-fold increase in the interlaminar peel strength of treated Kevlar 49–epoxy composites with failure mode changes from interface failure to mixtures of fibre and matrix failure. Using a wet chemical reaction approach, Wu and Tesoro [43] have been able to incorporate amine functional groups on the fibre surface by bromination followed by ammonolysis, nitration, and reduction. They have reported results similar to those of Allred *et al.*

5. Aramid–epoxy interphase

Most previous attempts at elucidating the relation between molecular structures and adhesion have followed either of two approaches. One approach deals with the microstructural aspects of bond forming and concentrates on the chemistry and physics of the interphase. The other approach deals with the macrostructural aspects and mechanical analysis of the interphase.

5.1. Microstructural aspects of bond forming

Microstructural aspects of polymer–polymer adhesion have been discussed by Allen [44]. He has explained several mechanisms for polymer–polymer bonding, each involving combinations of physical and chemical interactions. These mechanisms are: mechanical interlocking, adsorption interactions, electrostatic interactions, and interdiffusion of the polymer chain segments.

5.1.1. Mechanical interlocking

Mechanical interlocking of two adherants is the result of interpenetration at surface irregularities and molecular contacts. These surface irregularities act as mechanical anchors, and high bond strengths can be obtained even though other interactions may be weak. This mechanism has a profound influence on the adhesion of polymers to porous materials such as wood, textiles, and metal oxides, but for the microscopically smooth surfaces of aramid fibres, mechanical interlocking is not expected to be significant.

5.1.2. Adsorption interactions

Adsorption interactions refer to processes whereby the molecules of one phase are attracted to specific sites on the other phase. These attractive forces originate from basic chemical interactions, covalent chemical bonds and secondary chemical interactions. Covalent bonds involve sharing of electrons among atoms, and are the primary form of chemical interactions (163 to 465 $\mathrm{kJ\,mol^{-1}}$). Secondary interactions involve electron correlation between molecules and are much weaker chemical interactions (8 to 25 $\mathrm{kJ\,mol^{-1}}$). Secondary interactions include non-polar dispersion forces (Van der Waals forces), polar–dipole interactions, and polar Lewis acid/base interactions (including hydrogen bonding). All types of adsorption interactions require intimate physical contact between the molecules of the two phases but secondary interactions are effective over greater atomic distances than covalent interactions and are a prerequisite for covalent interactions. To achieve a stable interface, formation of covalent bonds at the interface is very desirable.

The results reported by Allred *et al.* [42] and Wu and Tesoro [43] on a two-fold increase in interlaminar peel strength of aramid composites by forming chemically active groups on the fibre surface was attributed to the formation of covalent bonds. Timm *et al.* [45] reported the possibility of chemical reactivity of the secondary aromatic amines in Kevlar 49, especially in anhydride cured epoxies. Using FTIR techniques, Garton and Daly [46] examined the interface of a model PPTA surface with both anhydride- and amine-cured DGEBA epoxy. For the aromatic amine-cured epoxy, no significant effect from PPTA on the cross-linking was observed; however, for the anhydride-cured epoxy the effect of the aramid surface was significant. Garton and Daly determined that the changes in the anhydride system were due to reactions with adsorbed water, although they did not reject the possibility that the amide functionality of the aramid may play a more significant role at high temperatures. Using photoacoustic FTIR spectroscopy, Chatzi *et al.* [47] determined that 30% of the N–H groups in Kevlar

49 fibres may be accessible for possible reactions, but the other 70% are sterically inaccessible.

5.1.3. *Electrostatic attractions*

Electrostatic attractions can result from transfer of electrons across the interface, which create positive and negative charges that attract each other. Electrostatic interactions are usually significant in metal–polymer and fine particle adhesion, but for the polymers electrostatic forces are usually small compared to other types of interactions. Inverse gas chromatography studies by Chappell and Williams [48], has shown that extracting the anti-static sizing of the Kevlar 49 fibres increases the dispersive component of the surface-free energy from 33.3 to 54.1 $\mathrm{mN\,m^{-1}}$. In the absence of perturbation from other types of interactions, the electrostatic interactions could become significant to the aramid adhesion.

5.1.4. *Polymer interdiffusion*

The contribution of interdiffusion in polymer–polymer adhesion has long been recognized [49]. The extent of diffusion of one polymer phase into another phase depends on their mutual molecular affinities. For aramid–epoxy adhesion, polymer interdiffusion is not possible, but macroscopic diffusion of the epoxy constituents into the fibre skin and between or within fibrils is possible.

5.2. Macrostructural properties

Macrostructural properties of the adhering phases have pronounced effects on the strength of their interphase. Mechanisms of adhesion are influenced by bulk and surface properties such as mechanical interactions, wetting, and weak boundary layers. These properties do not directly create interfacial bonding, but they can enhance or weaken any of the possible adhesion mechanisms.

5.2.1. *Mechanical interactions*

Mechanical interactions have several origins including surface topography, thermal stresses, and Poisson contraction.

The surface topography of the contacting solids is very important to their adhesion. Solid surfaces are generally rough on a microscale. When two solid surfaces are in direct contact, the actual area of molecular contact is limited to a relatively few high points on each surface. A low contact area results in limited interactions and weak adhesion. In liquid–solid adhesion, for low-viscosity liquids that can conform to the surface of the solid, the increase in the surface area due to the surface roughness improves all adhesion mechanisms. Breznick *et al.* [41] have reported a 20% interlaminar shear improvement for roughened aramid fibres, however, there was a 15% loss of fibre strength. Conversely, when the liquid has high viscosity or high surface tension, it can form bridges over the rough surfaces and create voids. The presence of voids or bubbles at the fibre–matrix interface is generally detrimental to good adhesion.

The effects of surface topography can be analysed in terms of frictional forces. Both adhesion and deformation contribute to friction. The adhesion contribution is due to rupture of molecular bonds that takes place during friction and involves local motions of order of 1 nm. The deformation contribution is due to mechanical interactions of the two surfaces and involves motions exceeding 1 μm. Friction from surface deformations is always present even when there is no adhesion. For instance, when an inert lubricant is interposed between the two surfaces, the adhesion friction is eliminated, but there are still deformation frictions [50].

Pull-out techniques to determine the interfacial adhesion either explicitly or implicitly include the effects of friction. Piggott *et al.* [51] have reported on pull-out experiments with carbon and glass fibres. Their results suggest that the normal pressures and coefficients of interfacial friction are more dependent on the state of cure than the type of resin used. Their reported values for the coefficient of friction of carbon fibres vary from 0.42 to 0.58, with the higher value corresponding to the higher curing temperatures. The reported values for aramid fibres [3] vary from 0.41 to 0.46, which suggests a similarity of its surface topography to that of carbon fibres. The presence of a coating on the fibre can significantly affect the friction by modifying the surface topography. The compilation of pull-out properties of coated Kevlar fibres by Mai and Castino [52] has demonstrated that shearing rate and interfacial viscosity can significantly affect the interfacial friction of the coated fibres.

Reedy [53] has reported on a finite element analysis of stress concentrations at the Kevlar–epoxy interface. Comparing computed frictional stresses with the experimental data, Reedy has suggested that for Kevlar 49 fibres the friction due to deformation has a magnitude of roughly 50% of that due to adhesion. Reedy has also suggested that when debonding occurs, the results of a linear elastic, perfectly bonded fibre–matrix model are no longer applicable. Shih and Ebert [54] have presented a theoretical model to describe the effects of the interface on the tensile strength of unidirectional composites. Their model suggests that the frictional component of adhesion can significantly affect the tensile strength of the composite.

Thermal stresses are caused by dimensional shrinkage of the resin around the fibre. Cooling, solvent removal, and chemical reactions can cause shrinkage. Thermal stresses can increase surface contact and enhance frictional interactions, but they can also cause elastic strains, which upon debonding, act as a locus of failure. For composites, the thermal stresses are mainly due to the difference in the thermal expansion properties of the fibres and the matrix. Anisotropic aramid and carbon fibres have different thermal expansion coefficients in their axial and radial directions. During cool-down from high curing temperatures, the mismatch between matrix and fibre shrinkage can result in radial and axial stresses. Nairn and Zoller [55] have discussed the effects of thermal stresses on Kevlar and carbon composites made with epoxies, amorphous thermoplastics, and semicrystalline thermoplastics. They conclude that any matrix-dependent composite property is affected by the thermal stresses.

Rojstaczer *et al.* [56] have reported on the thermal expansion properties of aramid fibres. For Kevlar 49 fibres, they have reported an axial thermal expansion coefficient of -5.7 p.p.m. $^\circ C^{-1}$, which is different from the -2 p.p.m. $^\circ C^{-1}$ value reported by the manufacturer [3]. A negative thermal expansion coefficient indicates shrinkage with increasing temperature. The off-axis mechanical properties of the fibres are very difficult to determine and are often extracted from the composite properties. These calculations usually ignore the effects of adhesion on the thermomechanical properties. Based on a matrix thermal expansion of 65 p.p.m. $^\circ C^{-1}$ and a Poisson's ratio of 0.35 for both matrix and fibres, Rojstaczer *et al.* [56] have reported a value of 66.3 p.p.m. $^\circ C^{-1}$ for the radial thermal expansion coefficient of Kevlar 49 fibres.

For carbon fibres, the reported thermal expansion coefficients are -0.1 to -0.5 p.p.m. $^\circ C^{-1}$ for axial and 7 to 12 p.p.m. $^\circ C^{-1}$ for the radial expansions [57]. Because most polymer matrices have thermal expansion coefficients of 60 to 75 p.p.m. $^\circ C^{-1}$, it can be inferred that along the radial directions, the thermal shrinkage mismatch between fibre and matrix is much larger for carbon composites than for aramid composites. Comparing carbon and aramid fibres, Penn *et al.* [58] have suggested the lower level of thermal stresses in aramid composites as an important reason for their relatively weaker interfacial adhesion.

Poisson's ratio differences between fibres and matrix can result in interfacial stresses similar to thermal stresses. When a fibre has a lower axial Poisson's ratio than the matrix, upon application of axial tension to the composite the matrix shrinks to a greater extent than the fibre, resulting in radial compressive stresses. This compressive load can increase the interfacial surface contact and bonding. Conversely, upon compression, the Poisson's ratio mismatch can contribute to fibre–matrix debonding.

Axial Poisson's ratio of the polyaramid fibres has been back-calculated from their composite properties [59] and is determined to be about 0.35. Direct measurement of the fibre Poisson's ratio is not reported in the literature. For carbon fibres, the reported values of axial Poisson's ratios are 0.22 to 0.25 [59] and for epoxy matrices the Poisson's ratio varies between 0.33 and 0.40. The mismatch of Poisson's ratio between fibre and matrix is much greater for carbon fibres than aramid fibres, suggesting greater normal compressive stresses for the carbon composite under tension. There is also the possibility that the Poisson's ratio of the aramid fibre is larger than the epoxy matrix, in that case Poisson's ratio mismatch can contribute to fibre–matrix debonding. Drzal [60], in comparing the interfacial behaviour of aramid and carbon composite, has suggested that both the low thermal and Poisson's ratio mismatch of aramid–epoxy as well as the fibre fibrillar microstructure are adversely affecting the aramid–epoxy adhesion.

5.2.2. Wetting

Adequate wetting of the fibre surface by liquid resin is a prerequisite for good adhesion. The importance of wetting in adhesion has been dramatically demonstrated by Sharpe *et al.* [61]. When liquid epoxy was cured on solid polyethylene, the adhesion was low, however, solidification of molten polyethylene on the cured epoxy produced a much stronger adhesion. In the first case, the liquid epoxy with high surface tension does not wet the solid polyethylene with low surface tension; but in the second case, liquid polyethylene with low surface tension could wet and spread over high surface tension solid epoxy.

Li *et al.* [62] have studied the wettability of carbon and aramid fibres by both the Wihelmy and the solidification front techniques. The Wihelmy technique yielded 42.4 and 43.7 $mN\,m^{-1}$ values for the surface energies of carbon and aramid fibres, respectively. Solidification front measurement resulted in 41.8 and 46.4 $mN\,m^{-1}$ for carbon and aramid fibres, respectively. Using contact angle analysis, Penn *et al.* [58] have also determined similar surface energies for carbon and aramid fibres. A report by Wesson and Allred [63] has shown that surface energies of aramid fibres and liquid. Diglycidal ether of bisphenol A (DGEBA) epoxy resins are also similar. From these results, both carbon and aramid fibres are expected to have similar "good" thermodynamic wetting with liquid epoxies.

5.2.3. Weak boundary layers

Weak boundary layers refer to layers in the interphase with lower cohesive or adhesive properties than their bulk substrates. Weak boundary layers can be due to entrapped gas, contaminants, and structural anomalies of the substrates. They are generally detrimental to adhesion and can prevent the formation of strong adhesion even though extensive interfacial contact might be present.

There are two types of weak boundary layers, adhesive and cohesive. With an adhesive weak boundary layer, the fibre–matrix interface fails with little damage to either fibre or matrix, but with a cohesive weak boundary layer, one or both are involved in failure. Both types of weak boundary layers can coexist, but depending on the mechanical state of stresses, the effect of one can mask the other.

For aramid fibres, the possibility of a cohesive weak boundary layers exists. The skin–core morphology of the aramid fibres could result in weaker properties in the surface region of the fibre. Upon application of shear to the fibre surface, cracks could be generated in the skin region producing an inefficient fibre–matrix load transfer.

There are indications that surface treatments that do not affect the aramid surface morphology are ineffective in improving its epoxy adhesion. Penn *et al.* [39], have applied various coupling agents to promote aramid–epoxy adhesion and have reported no significant changes in the fibre–matrix bond strength. In a more recent study by Penn *et al.* [64], flexible reactive pendent groups have been covalently attached to the aramid fibre surface, but no mechanical improvement of interfacial bonding was observed. Penn has attributed this observation to a lack of bonding between the pendent groups and the matrix; however, failure in a cohesive weak boundary layer could be another explanation.

Theoretical and experimental studies of the aramid fibres' mechanical properties suggest the possible adverse effects attributable to the aramid skin–core morphology. Data given by Kompaniets *et al.* [65] have demonstrated that for the aramid fibres the fibre tensile strength is gauge-length dependent, but for the unidirectional composites the tensile strength is independent of the gauge length. This observation suggests a different failure mode for the embedded fibres which experience the load transfer by interfacial shear. Fibre pull-out experiments by Miller *et al.* [66] do not suggest any difference between bond strength of "as-received" and "acetone-washed" aramid fibres. As-received fibres have a sizing on them which should introduce an adhesive weak boundary layer, yet the fibre–matrix bond strength is unaffected. Based on statistical methods to examine the effect of fibre dimensions on the ultimate properties of crystalline polymers, Wagner [67] has suggested that for the Kevlar fibres surface flaws may be responsible for initiation of the fibre fractures. A theoretical study of the elastic extension of an aramid fibre by Northolt and Hout [68] has shown that the initial orientation of the crystallites and shear modulus parallel to the chain direction can significantly affect stress build up during fibre extension. The skin–core morphology in the aramid can thus result in non-uniform stress build up within the fibre during its extension. The anisotropy of fibre morphology can also result in non-uniform thermal stress distributions within the fibre during composite curing [69]. Thus far, the effect of the skin–core morphology of aramid fibres on its adhesion properties has not been fully investigated.

6. Conclusion

The composite interphase can significantly affect the mechanical and thermal properties of the composite. For example, off-axis properties are generally improved by increasing interfacial bonding, while fracture toughness and impact resistance usually increase at low adhesion levels. The adhesion levels achieved between aramid fibres and epoxy matrices are much lower than those obtained by other inorganic reinforcing fibres. A combination of aramid fibre chemical and physical properties as well as its morphology are responsible for the relatively low aramid–epoxy adhesion. Aramid–epoxy chemical interactions are expected to be only the weak secondary type but strong enough to result in a "good" thermodynamic wetting of the fibre. Fibre–matrix physical interactions which result from thermal stress and Poisson contraction are not expected to be high enough to improve significantly interfacial load transfer efficiency and may even be detrimental to the adhesion. Skin–core morphology of the aramid fibres may result in weaker properties in the surface region which can lead to a cohesive weak boundary in the fibre–matrix interphase. These observations suggest that to improve aramid–epoxy adhesion both the morphological and the physiochemical modification of the interphase must be considered.

References

1. T. TAKATA, *Sen-I-Gakkaihi* **44**(2) (1987) 67 (translation from Japanese).
2. R. J. MORGAN and R. E. ALLRED, "Reference Book for Composites Tech.," edited by S. M. Lee (Technomic, Lancaster, PA, 1989) p. 143.
3. C. C. CHIAO and T. T. CHIAO, in "Handbook of Composites" edited by G. Lubin (Van Nostrand Reinhold, New York, 1982) p. 272.
4. E. G. CHATZI and J. L. KOENIG, *Polym. Plast. Technol. Engng* **26** (1987) 229.
5. P. S. THEOCARIS, "The Mesophase Concept in Composites" (Springer-Verlag, Berlin, 1987).
6. L. T. DRZAL, *J. Adhesion* **16** (1983) 1.
7. B. D. AGARWAL and L. J. BROUTMAN, "Analysis and Performance of Fiber Reinforced Polymers" (Wiley, New York, 1980) p. 15.
8. L. T. DRZAL, M. J. RICH and S. SUBRAMONEY, in "Proceedings of the Third Annual Conference on Advanced Composites", Detroit, September 1987 (ASM, Detroit, 1987) p. 305.
9. M. J. OWEN, in "Fracture and Fatigue" edited by L. J. Broutman, (Academic Press, New York, 1974) p. 341.
10. P. W. M. PETERS and G. S. SPRINGER, *J. Compos. Mater.* **21** (1987) 157.
11. J. CHANG, J. P. BELL and R. JOESEPH, *SAMPE Quart.* **18** (1987) 39.
12. Y. W. MAI and F. CASTINO, *J. Mater. Sci.* **19** (1984) 1638.
13. A. V. TOBOLSKY and H. F. MARK, "Polymer Science and Materials" (Wiley-Interscience, New York, 1971) p. 231.
14. Y. TERMONIA and P. SMITH, *Polymer* **27** (1986) 1845.
15. K. TAKAHO *et al.*, *J. Appl. Polym. Sci.* **32** (1986) 3133.
16. P. R. DVORNIC, *J. Polym. Sci. A* **24** (1986) 1133.
17. E. E. MAGAT, *Phil. Trans. R. Soc. Lond. A* **294** (1980) 463.
18. J. PRESTON, *Polym. Engng Sci.* **15** (1975) 199.
19. P. R. LANGSTON, in "Proceedings of the 32nd International SAMPE Symposium", April 1987 edited by R. Carlon, M. Burg, K. J. Kroller and F. J. Riel (SAMPE, Covina CA, 1987) p. 1399.
20. "Kevlar Composites" (Technology Conferences, El Segundo, California, 1980).
21. P. G. RIEWALD, A. K. DHINGRA and T. S. CHERN, in "Proceedings of ICCM and ECCM VI", London, July 1987 (Elsevier Applied Science, London, 1987) p. 5.362.
22. M. G. DOBB, D. J. JOHNSON and B. P. SAVILLE, *J. Polym. Sci. B* **15** (1977) 2201.
23. R. J. MORGAN, C. O. PRUNEDA and W. J. STEELE, *ibid.* **21** (1983) 1757.
24. I. M. BROWN, T. C. SANDRECZKI and R. J. MORGAN, *Polymer* **25** (1984) 759.
25. L. S. LI, L. F. ALLARD and W. C. BIGELOW, *J. Macromol. Sci. Phys.* **B22** (1983) 269.
26. E. G. CHATZI, M. W. URBAN and J. L. KOENIG, *Makromol. Chem. Macromal. Symp.* **5** (1986) 99.
27. H. H. YANG, M. P. CHOUINARD and W. J. LINGG, *J. Appl. Polym. Sci.* **34** (1987) 1399.
28. A. M. TIEFENTHALER and M. W. URBAN, *Appl. Spectrosc.* **42** (1988) 163.
29. R. J. MORGAN and C. O. PRUNEDA, *Polymer* **28** (1987) 340.
30. L. PENN and F. LARSEN, *J. Appl. Polym. Sci.* **23** (1979) 59.
31. W. B. WHALLEY, B. J. SMITH and J. P. GREEVY, *J. Mater. Sci. Lett.* **5** (1986) 342.
32. J. S. LEE, J. F. FELLERS and M. Y. TANG, *J. Compos. Mater.* **19** (1985) 114.
33. E. ASHBEE and K. H. G. ASHBEE, *J. Mater. Sci. Lett.* **4** (1985) 249.
34. H. H. MITTELMAN, I. ROMAN and G. MAROM, *ibid.* **4** (1985) 1361.
35. P. A. SMITH, D. G. GILBERT and A. POURSARTIP, *ibid.* **4** (1985) 845.
36. D. M. RIGGS, R. J. SHUFORD and R. W. LEWIS,

"Handbook of Composites" (Van Nostrand Reinhold, New York, 1982) p. 196.

37. L. T. DRZAL, *J. Adhesion* **16** (1983) 133.
38. T. F. COOKE, *J. Polym. Engng* **7** (1987) 197.
39. L. S. PENN, F. A. BYSTRY and H. MARCHIONNI, *Polym. Compos.* **4**(1) (1983) 27.
40. M. R. WERTHEIMER and H. P. SCHREIBER, *J. Appl. Polym. Sci.* **26** (1981) 2087.
41. M. BREZNICK *et al., Polym. Commun.* **28** (1987) 55.
42. R. E. ALLRED, E. W. MERRILL and D. K. ROYLANCE, "Molecular Characterization of Composite Interfaces" (Plenum Press, New York, 1985) p. 333.
43. Y. WU and G. C. TESORO, *J. Appl. Polym. Sci.* **31** (1986) 1041.
44. K. W. ALLEN, *J. Adhesion* **21** (1987) 261.
45. D. C. TIMM, A. J. AYORINDE and C. H. LEE, *Polym. Engng Sci.* **24** (1984) 930.
46. A. GARTON and J. H. DALY, *Polym. Compos.* **6** (1985) 195.
47. E. G. CHATZI, M. W. URBAN and J. L. KOENIG, *Polymer* **27** (1986) 1850.
48. P. J. C. CHAPPELL and D. R. WILLIAMS, in "Proceedings of ICCM and ECCM VI", London, July 1987 edited by F. L. Matthews, N. C. R. Buskell, J. M. Hodgkinson and J. Morton (Elsevier Applied Science, London, 1987) p. 5.346.
49. S. S. VOYUTSKII, "Autohesion and Adhesion of High Polymers" (Wiley Interscience, New York, 1963).
50. B. W. CHERRY, "Polymer Surfaces" (Cambridge University Press, Cambridge, 1981) p. 95.
51. M. R. PIGGOTT, P. S. CHUA and D. ANDISON, *Polym. Compos.* **6** (1985) 242.
52. Y. W. MAI and F. CASTINO, *J. Mater. Sci. Lett.* **4** (1985) 505.
53. E. D. REEDY, *J. Compos. Mater.* **19** (1985) 533.
54. G. C. SHIH and L. J. EBERT, *ibid.* **21** (1987) 207.
55. J. A. NAIRN and P. ZOLLER, *J. Mater. Sci.* **20** (1985) 355.
56. S. ROJSTACZER, D. COHN and G. MAROM, *J. Mater. Sci. Lett.* **4** (1985) 1233.
57. D. HULL, "An Introduction to Composite Materials" (Cambridge University Press, Cambridge, 1981) p. 14.
58. L. S. PENN *et al., Polym. Sci. Technol.* **27** (1985) 93.
59. "Fiber Composite Analysis and Design", Vol. 1, "Composite Materials and Laminates" (US Department of Transportation, Federal Aviation Administration, 1984).
60. L. T. DRZAL, *SAMPE J.* **19** (5) (1983) 7.
61. L. H. SHARPE, H. SCHONHORN and R. F. GOULD, in "Contact Angle, Wettability and Adhesion" edited by R. F. Gould (ACS, Washington D.C., 1964) p. 189.
62. S. K. LI, R. P. SMITH and A. W. NEUMANN, *J. Adhesion* **17** (1984) 105.
63. S. P. WESSON and R. E. ALLRED, in "Proceedings of the 7th Annual Meeting of the Adhesion Society", Jacksonville, Florida, 1984 (Adhesion Society, Akron, Ohio, 1984) p. 27.
64. L. S. PENN, T. J. BYERLEY and T. K. LIAO, *J. Adhesion* **23** (1987) 163.
65. L. V. KOMPANIETS *et al., Polym. Compos.* **6** (1985) 54.
66. B. MILLER, P. MURI and L. REBENFELD, *Compos. Sci. Technol.* **28** (1987) 17.
67. H. D. WAGNER, in "Proceedings of ICCM and ECCM VI", London, July 1987 edited by F. L. Matthews, N. C. R. Buskell, J. M. Hodgkinson and J. Morten (Elsevier Applied Science, London, 1987) p. 5.517.
68. M. G. NORTHOLT and R. V. D. HOUT, *Polymer* **26** (1985) 310.
69. W. B. AVERY and C. T. HERAKOVICH, *J. Appl. Mech. Trans. ASME* **53** (1986) 751.

Received 22 June
and accepted 16 August 1989